



Detection of bubble nucleation event in superheated drop detector by the pressure sensor

MALA DAS* and NILANJAN BISWAS

Astroparticle Physics and Cosmology Division, Saha Institute of Nuclear Physics, Kolkata 700 064, India

*Corresponding author. E-mail: mala.das@saha.ac.in

MS received 25 August 2015; revised 6 April 2016; accepted 17 June 2016; published online 8 December 2016

Abstract. Superheated drop detector consisting of drops of superheated liquid suspended in polymer or gel matrix is of great demand, mainly because of its insensitivity to β -particles and γ -rays and also because of the low cost. The bubble nucleation event is detected by measuring the acoustic shock wave released during the nucleation process. The present work demonstrates the detection of bubble nucleation events by using the pressure sensor. The associated circuits for the measurement are described in this article. The detection of events is verified by measuring the events with the acoustic sensor. The measurement was done using drops of various sizes to study the effect of the size of the drop on the pressure recovery time. Probability of detection of events has increased for larger size of the superheated drops and lesser volume of air in contact with the gel matrix. The exponential decay fitting to the pressure sensor signals shows the dead time for pressure recovery of such a drop detector to be a few microseconds.

Keywords. Bubble nucleation; pressure sensor; superheated liquid drop.

PACS Nos 07.07.Df; 07.64.+z; 29.40.-n

1. Introduction

Superheated drop detector (SDD) consists of a large number of micron-sized drops of superheated liquid dispersed homogeneously in a viscoelastic ultrasound gel or polymer matrix [1,2]. Each drop can be considered as a micron-sized bubble chamber, where a drop vapourizes (that is, phase transition or nucleation occurs) when sufficient energy is deposited by some incident energetic radiation, e.g. neutrons, γ -rays, charged particles, etc. under certain operating conditions. The main advantage of this type of detector is that it can be made sensitive to neutrons and insensitive to γ -rays and other lower ionizing radiations (like β -particles) by controlling the operating temperature and/or pressure. This property of the detector makes it an important tool in neutron dose measurement in a γ -ray background. This type of detector has widespread applications in different fields, e.g. in neutron dosimetry [3], γ -ray [4] and heavy ions [5] detection, in space science [6], in medical physics [7] and in dark matter search [8–10]. The change from metastable superheated state to a stable vapour state starts with

the formation of a critical-sized vapour embryo. This is described by Seitz's thermal spike model [11], according to which as the radiation deposits energy along its path inside the superheated liquid, embryonic vapour bubbles are formed. If the radius of such a bubble is greater than the critical radius, then it expands very fast until the liquid drop vapourizes. The vapourization of a superheated drop to a bubble (event) is associated with a change in pressure and the emission of an acoustic pulse. The bubble nucleation is usually detected by measuring the acoustic signal using piezoelectric transducer which converts the acoustic pulse to the electrical signal. The active device for counting the number of bubble nucleation was described by digitizing the acoustic signals [12–14]. In the present work, the event detection has been done by measuring the pressure signals. The associated circuit for the measurement of pressure pulse during the nucleation event is described. The measurements were done for three different drop size distributions. The pressure sensor was calibrated by noting the voltage drop across the resistance with change in pressure in a system. The frequency response of the amplifier used to amplify

the pressure signal output was studied. The acoustic pulse of bubble nucleation has also been measured for verification. The fast Fourier transform (FFT) of the acoustic signals was performed to extract the frequencies associated with bubble nucleation events due to the background. The dead time for pressure recovery for the nucleation event was investigated for drops of various sizes.

2. Experimental details

The SDD was prepared by suspending superheated liquid drops of R12 (CCl_2F_2 , boiling point: -29.8°C) in the aquasonic gel matrix. The liquid R12 was added to the degassed gel in a high-pressure autoclave containing the magnetically coupled stirrer (Amar Equipments Pvt. Ltd, No. 1314). Drops of different broad size distributions were fabricated by varying the stirrer rotation speeds to 1400 RPM, 700 RPM and 300 RPM. Drops of diameters in the range of about $1\ \mu\text{m}$ to about $500\ \mu\text{m}$ were created by this process. The SDD thus prepared was taken in a borocil glass container.

The experimental set-up is shown in figure 1. The acoustic sensor is a wideband AE amplifier sensor (WSa, Physical Acoustics Corporation) and the pressure sensor is a pressure transmitter (WIKA R1, Wika Instruments Ltd). The acoustic sensor was placed below the detector container, in contact with its bottom surface, coupled with aquasonic gel. The pulses from the pressure sensor were too low to be measured and

therefore were amplified using an IC, OP27 circuit as shown in figure 2. Here, the OP27 Amplifier was used in ‘non-inverting’ mode with a voltage gain of 11. The resistors used in the circuit are general purpose carbon film resistors of 0.25 W with a tolerance level of $\pm 5\%$. The temperature coefficient is about 0 to $-450\ \text{PPM}/^\circ\text{C}$. The effect of temperature on the resistors has been neglected and the experiment was done at room temperature ($20\text{--}25^\circ\text{C}$). The noise amplitude generally remains in the range of 10–20 mV (peak-to-peak) at the laboratory and its frequency lies in the range below 1 kHz. This noise level does not affect the characteristics or performance of the sensor–amplifier system. The fluctuation in the measurement of output amplitude was about 10 mV. The measured frequency response curve of the amplifier, OP27, used in this experiment is shown in figure 3. The circles are measured values and the dotted line is connecting the points. From the frequency response curve shown in figure 3, it is observed that the bandwidth (BW) of the amplifier is about 10 Hz to 620 kHz.

The pressure sensor was tested by measuring the variation of pressure in a 400 ml pressure chamber as shown in figure 4. The pressure inside the pressure chamber was generated by connecting the chamber with the refrigerant gas (R134a) container through a pressure pipe in valve-1 and then filling the container with the gas. After applying a pressure of about 6.5 bar, the pressure was reduced manually in steps of 0.5 bars by opening the valve-1 and the corresponding voltage

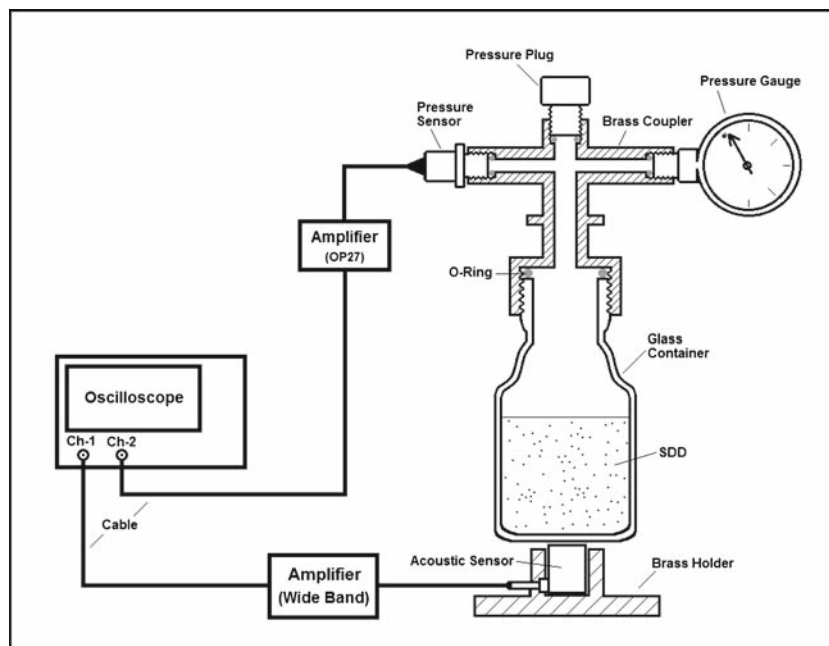


Figure 1. The experimental set-up for measuring the bubble nucleation event with pressure and acoustic sensors.

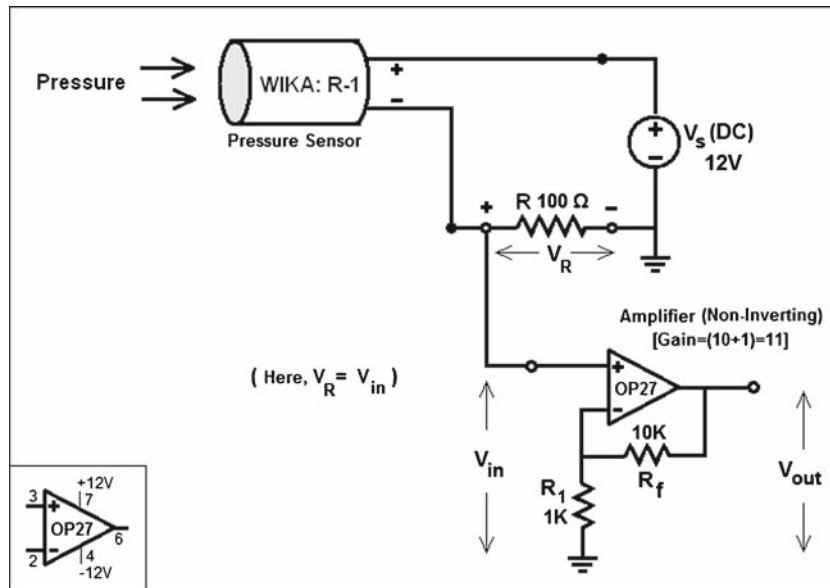


Figure 2. The pressure pulse measurement circuit with the pressure sensor.

readings of the Amplifier (OP27) input and output were noted by using the multimeter.

With the tested pressure sensor and the amplifier, the bubble nucleation events due to the background were detected by measuring both the pressure signal and the acoustic signal of each nucleation event and observed in 350 MHz, 2 GSa/s, 16 bit, mixed signal oscilloscope. The measurements were done separately with the SDDs prepared with three different RPMs. The space between the pressure sensor and the detector matrix was initially filled with air. To test whether the events were missed by the pressure sensor, this space was filled with glycerol and finally with aquasonic gel

matrix of the detector. The measurements were taken for all these configurations and simultaneously both with the acoustic sensor and the pressure sensor.

3. Results and discussions

The pressure–voltage calibration data of the pressure sensor are shown in figure 5 in symbols where the solid line is the straight line fittings to the data. The background data saved in CRO are plotted with time (in seconds) along the *x*-axis and amplitude of the pulse (in volt) along the *y*-axis. The FFT of the acoustic

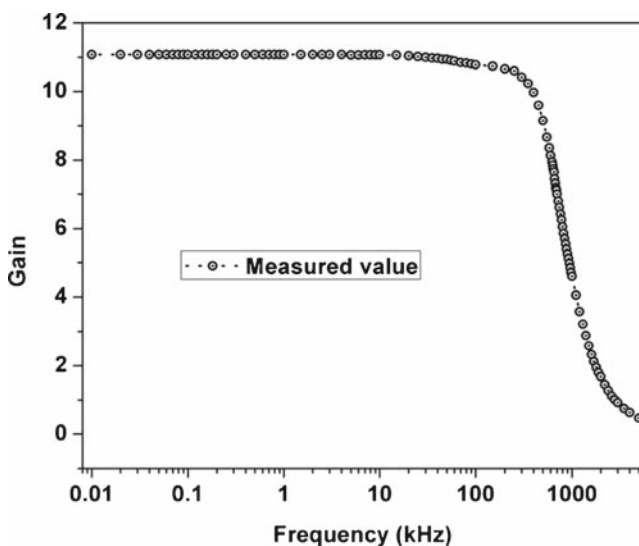


Figure 3. The measured frequency response curve of OP27.

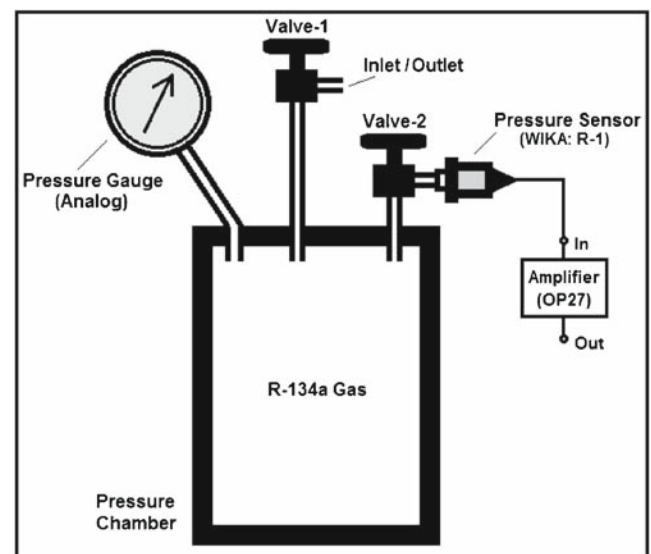


Figure 4. Block diagram of the set-up for testing the pressure sensor with varying pressure.

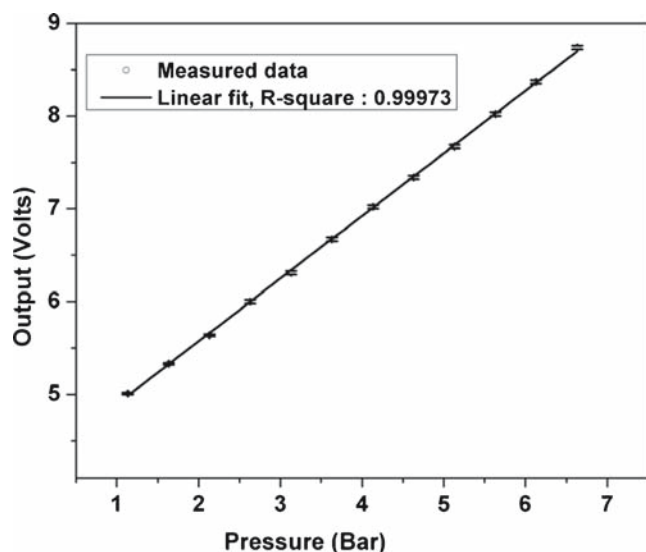


Figure 5. The measured pressure–voltage calibration curve of the pressure sensor.

signals was performed which provides the frequencies associated with the sound emitted during the bubble nucleation process. The decaying parts of the pressure pulses were fitted with the exponential decay function to extract the time of recovery of each nucleation event, which is the dead time of the device for the pressure recovery.

The drop size distributions for the three different rotation speeds of the stirrer, 1400 RPM, 700 RPM and 300 RPM are shown in figure 6. A typical signal output from the pressure sensor due to one bubble nucleation event is shown in figure 7. The measurement shows that the probability of detection of events by the sensors

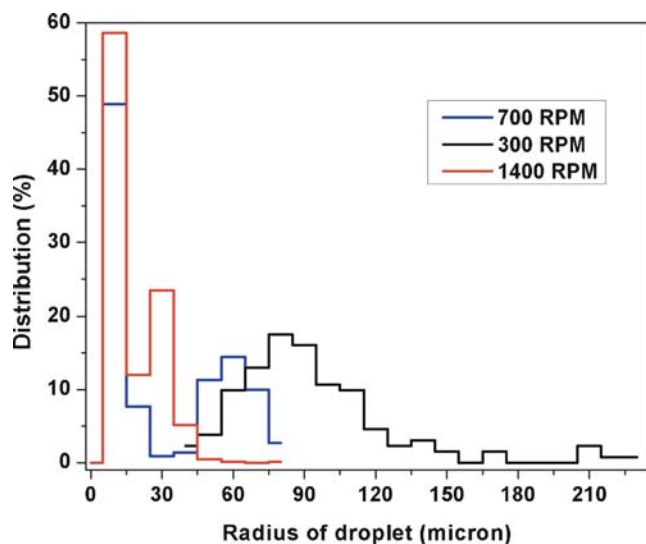


Figure 6. The drop size distributions for 1400 RPM, 700 RPM and 300 RPM.

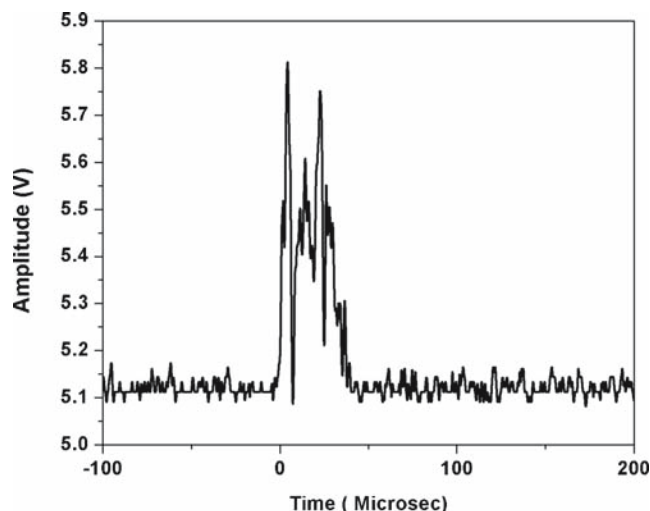


Figure 7. A typical signal output from the pressure sensor.

increases as the drop size increases. With the air gap between the pressure sensor and the detector matrix, a few events were observed to be missed by the pressure sensor but detected by the acoustic sensor. As an example, 16.7% pressure pulses were missed for 700 RPM droplets with 11 cm air gap. Almost all events were detected while the above space was filled with aquasonic gel. The pressure change during one nucleation event is observed to be about 1 bar. A typical FFT plot of one such acoustic pulse to an event is shown in figure 8. FFT of the acoustic pulses show that the range of frequency is in few kHz to about 1 MHz with several harmonics. The decay part of one of the pressure pulses as recorded by the pressure sensor is shown in figure 9. The decay time constant of the pressure pulse varies from about $1 \mu\text{s}$ to about $20 \mu\text{s}$ for different drop sizes. The total pressure recovery takes place at a maximum

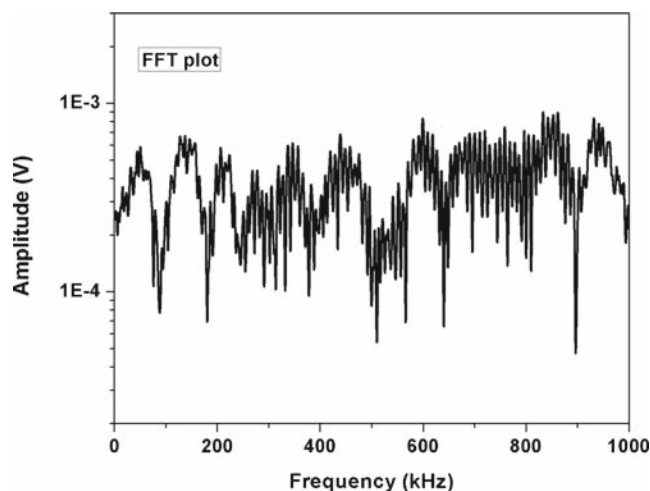


Figure 8. A typical FFT plot of one of the acoustic pulses to an event.

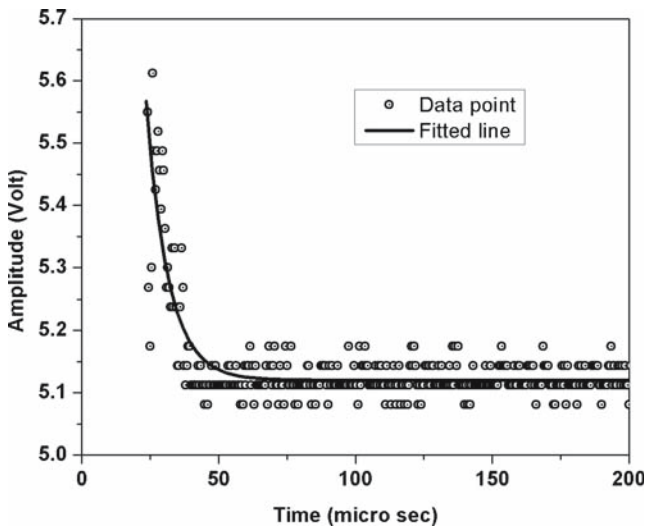


Figure 9. The decay part of the pressure pulse data as recorded from the pressure sensor. The solid line is the exponential fitting to the data.

of about $50 \mu\text{s}$ after each nucleation event, which is the dead time for pressure recovery of such a detector system. The decay time is not observed to be dependent on drop diameter in the present investigation but the pressure pulses become more detectable with the increase of the drop size, that is, about 38% more from 300 RPM droplets than from 700 RPM droplets.

4. Conclusion

The present work demonstrates the detection of bubble nucleation events in superheated drop detector by using the pressure sensor with varying drop size distributions in the range of about $10\text{--}230 \mu\text{m}$. Greater number of

events has been detected for larger size of the superheated drops and lesser volume of air in contact with the aquasonic gel matrix in which the drops were suspended. Best results have been obtained with the gel matrix filling the entire volume of the detector container. The FFT of the acoustic signals shows the wide band frequencies released during the bubble formation process and the exponential decay fitting to the pressure signals shows the dead time for pressure recovery of such detector as a few microseconds.

References

- [1] R E Apfel, *U.S. Patent* **4**, 143 (1979)
- [2] H Ing and H C Birnboim, *Nucl. Tracks Radiat. Meas.* **8**, 285 (1984)
- [3] R E Apfel and S C Roy, *Nucl. Instrum. Methods* **219**, 582 (1984)
- [4] H Ing, R A Noulty and T D Mclean, *Radiat. Meas.* **27**, 1 (1997)
- [5] S L Guo, L Li, H Y Guo, C Q Tu, Y L Wang, T Doke, T Kato, K Ozaki, A Kyan, Y Piao and T Murakami, *Radiat. Meas.* **31**, 167 (1999)
- [6] H Ing and A Mortimer, *Adv. Space Res.* **14**, 73 (1994)
- [7] F d'Errico, R Nath, S K Holland, M Lamba, S Patz and M J Rivard, *Nucl. Instrum. Methods A* **476**, 113 (2002)
- [8] COUPP Collaboration: E Behnke *et al*, *Phys. Rev. Lett.* **106**, 021303 (2011)
- [9] PICASSO Collaboration: S Archambault *et al*, *Phys. Lett. B* **711**, 153 (2012)
- [10] SIMPLE Collaboration: M Felizardo *et al*, *Phys. Rev. Lett.* **105**, 211301 (2010)
- [11] F Seitz, *Phys. Fluids* **1**, 2 (1958)
- [12] R E Apfel and S C Roy, *Rev. Sci. Instrum.* **54**, 1397 (1983)
- [13] I Murai and T Sawamura, *Nucl. Instrum. Methods A* **547**, 450 (2005)
- [14] M Das, A S Arya, C Marick, D Kanjilal and S Saha, *Rev. Sci. Instrum.* **79**, 113301(1–6) (2008)